# Specific Volume of Deuterium Oxide from 2° to 40°C and 0 to 1000 Bars Applied Pressure

**Robert T. Emmet[1] and Frank J. Millero[2]**
*Rosenstiel School of Marine and Atmospheric Sciences, University of Miami, Miami, Fla. 33149*

**Direct measurements of the specific volume of deuterium oxide ($D_2O$) solutions were made with a magnetic float densimeter from 2° to 40°C and from 0 to 1000 bars applied pressure. The results were fitted to a second degree secant bulk modulus equation: $(V^0P)/(V^0 - V^P) = A_0 + A_1P + A_2P^2 + CP^2$ where $V^0$ and $V^P$ are the specific volumes at zero and $P$ applied pressure, $A_0 = 1/\beta^0$ the reciprocal of the 1 atm compressibilities, and $A_1$ and $A_2$ are temperature dependent parameters. The specific volumes were fitted to this equation with a standard deviation of 6 ppm over the entire pressure and temperature range. The equation of state of $D_2O$ was used to compute several thermodynamic properties that are compared to the results obtained by other workers from 5° to 40°C and 0 to 1000 bars.**

One method of studying the structure of liquid water has been to examine the relative thermodynamic properties of water ($H_2O$) and deuterium oxide ($D_2O$) as functions of temperature and pressure and to suggest microscopic explanations for the differences.

Expressing a property as a function of mole fraction of deuterium is particularly revealing because it describes the effect of a definite microscopic feature, the mass of hydrogen. Properties of $D_2O$ and $H_2O$ differ because of the higher mass of the deuterium atom which results in the lower frequency for intramolecular vibrations for the O—D bond and the altered intermolecular forces (D—O. . .D—O) which are of more complex origin (*23*). The thermodynamic properties are related quantitatively to the microscopic systems through a partition function which sums contributions on all possible interactions. Difficulties arise in choosing the basic model or form of the function and the relative magnitude of the contributions within a given model. Partition functions have been derived by establishing a physical model, approximating it mathematically, and adjusting various parameters, such as the strength of the hydrogen bonds, so that the function, by means of statistical mechanics, will approximate the thermodynamic properties. Several widely differing theories have postulated models of water and have predicted the important properties with apparent success (*9, 18, 25*).

Kesselman (*12, 13*) and later Jůza et al. (*10*) have described the thermodynamic similarity of $H_2O$ and $D_2O$ in the region of higher temperature and pressure. Near the critical point the correlations are so good that properties of $D_2O$ can be accurately predicted from properties of $H_2O$ at the same reduced temperature and pressure. In the liquids, however, at lower temperatures and pressures where the physical behavior is not normal, the properties are not closely correlated. It is the purpose of this paper to accurately explore the *PVT* properties of $D_2O$ relative to $H_2O$ in the region 2–40°C and 0–1000 bars applied pressure.

[1] Present address, Naval Ship Research and Development Center, Annapolis, Md. 21402.
[2] To whom correspondence should be addressed.

By accurately measuring the specific volume of $D_2O$ relative to $H_2O$ and summarizing these results as equations of state in the following sections, various properties of $D_2O$ and $H_2O$ are calculated. The calculated relative specific heats show divergences as functions of temperature and pressure. If a prospective structural model is to be seriously considered, it must not only explain satisfactorily the phenomenon on which its formulation is based, but the rest of the outstanding puzzles of water as well. The specific heat behavior in particular is difficult to describe theoretically (*7*), and the functional patterns described here should present an exacting test for theoretical speculation.

## Experimental

***Apparatus.*** The high-pressure magnetic float densimeter used in this study is described in detail elsewhere (*16*). The high-pressure densimeter consists essentially of a 1 atm densimeter (*14*) enclosed in a nonmagnetic bomb with optical ports to observe the motion of the float. The apparatus consists of a pressure bomb, a magnetic float, and auxiliary measuring and control system.

The water used to calibrate the magnetic float densimeter was ion-exchanged 18 MΩ water (Millipore Super-Q System). The $D_2O$ was obtained from Mallinckrodt Chemical and had a minimum isotopic purity of 99.8%.

The pressure bomb used in this study was machined from Carpenter 20 stainless steel. The bomb is cylindrical with an inside diameter of 5.08 cm, an outside diameter of 12.70 cm, and a height of 19.05 cm. The top and bottom plugs of the bomb are seated with O-rings to form a vessel of 170 $cm^3$. The bottom plug contains an insert plug that supports a solenoid of 300 turns of No. 28 varnished magnet wire. The windows in the bomb were 30° cones machined from cast Plexiglas rod.

The magnetic float is made of thick wall (0.4 cm) pyrex glass and contains an Alnico-5 bar magnet (seated with Apiezon high-temperature wax or silastic R-T-V sealer). The volume of the float is 58.7672 $cm^3$ at 0°C and 1 atm (the weight is 57.62265 grams in vacuum).

The pressure bomb is completely immersed in a 30-liter constant temperature bath. The bath was controlled to ±0.001°C with a Hallikainen thermotrol. The temperature (IPTS-68) of the bath is set to ±0.005°C with a platinum resistance thermometer (calibrated by the National Bureau of Standards) and a G-2 Mueller bridge.

The pressure generating system was similar to that described elsewhere (*16*). A Harwood Engineering Co. dead weight tester was used to set and hold the pressure during a measurement. The mass of the floating weights of the piston gauge was multiplied by the local acceleration of gravity and divided by the measured area of the piston to give the pressure. The area was corrected for the film thickness and the effects of pressure to give pressures accurate to within ±0.1 at 1000 bars.

The electrical system is similar to the 1 atm densimeter and is described in detail elsewhere (*14, 16*).

***Calibration.*** The densimeter was calibrated (*3*) at various temperatures (0–40°C) and pressures (0–1000 bars) using

the densities of water derived from the sound-derived equation of state of Fine and Millero (*5*). The methods used to calibrate the densimeter are described in detail elsewhere (*14, 16*). By adding various platinum weights ($w$) to the magnetic float and measuring the hold down current ($i$), it is possible to determine the volume of the float ($V_f$) and the magnetic interaction constant ($f$) as a function of pressure and temperature

$$w\left(1 - \frac{d_{H_2O}}{d_{Pt}}\right) = -fxi + (V_f d_{H_2O} - W_f) \qquad (1)$$

where $d_{H_2O}$ is the density of water, $d_{Pt}$ is the density of platinum, and $W_f$ is the weight of the float.

The densimeter was calibrated at −2°, 0°, 2°, 4°, 6°, 8°, 10°, 15°, 20°, 25°, 30°, 35°, and 40°C at 100 bar intervals from 0 to 1000 bars (*3*). The 4°C calibration results are given in Table I. The average differences between the back-calculated densities and those used to calculate $V_f$ and $f$ are given in the last column of Table I. The average deviations in $d$ over the entire temperature and pressure range are within ±10 ppm (±3 ppm is the average) which is a measure of the precision of the density measurements.

## Results

The densities of $D_2O$ have been determined with the high-pressure magnetic float densimeter from 4° to 40°C and 0 to 1000 bars applied pressure. The experimentally determined specific volumes ($1/d$ in cm³/g) are given in Table II. The secant bulk modulus ($K$) was computed from these specific volumes using

$$K = \frac{V^0 P}{V^0 - V^P} \qquad (2)$$

A plot of $K$ vs. pressure is shown in Figure 1. As is quite apparent from this figure, $K$ is approximately a linear function of pressure, and the slopes are not strongly dependent on temperatures. We have, thus, first attempted to fit the $K$'s (using

**Table I. Calibration Results of High-Pressure Magnetic Float at 4°C**

| Press, bar | $d_{H_2O}$,[a] cm³ g⁻¹ | Equilibrium current,[b] amp | | | $V_f$, cm³ | $f$, g amp⁻¹ | $\Delta d$,[c] ppm |
|---|---|---|---|---|---|---|---|
| | | 0.50309, g | 0.74337, g | 0.98775, g | | | |
| 0.00 | 0.999972 | 0.121265 | 0.079763 | 0.037395 | 58.77212 | 5.5091 | 4.3 |
| 96.79 | 1.004710 | 0.156495 | 0.115038 | 0.072690 | 58.68854 | 5.5121 | 3.8 |
| 196.62 | 1.009490 | 0.191509 | 0.150133 | 0.107882 | 58.60371 | 5.5226 | 3.5 |
| 296.45 | 1.014164 | 0.225210 | 0.183904 | 0.141704 | 58.51855 | 5.5293 | 3.9 |
| 396.29 | 1.018735 | 0.257646 | 0.216362 | 0.174271 | 58.43369 | 5.5368 | 2.1 |
| 496.13 | 1.023207 | 0.288771 | 0.247572 | 0.205452 | 58.34745 | 5.5393 | 4.6 |
| 595.97 | 1.027581 | 0.318642 | 0.277527 | 0.235472 | 58.26263 | 5.5476 | 4.9 |
| 695.81 | 1.031861 | 0.347375 | 0.360293 | 0.264325 | 58.17774 | 5.5549 | 3.9 |
| 795.65 | 1.036048 | 0.374920 | 0.333870 | 0.291985 | 58.09255 | 5.5615 | 2.8 |
| 895.49 | 1.040146 | 0.401385 | 0.360366 | 0.318490 | 58.00575 | 5.5631 | 3.3 |
| 995.33 | 1.044155 | 0.426815 | 0.385770 | 0.343922 | 57.91797 | 5.5621 | 2.2 |

[a] Taken from Fine and Millero (*5*). [b] Equilibrium current for various masses on the float (reproducible to within 2 parts in $10^6$). Mass of the float is 57.62265 grams (in vacuum). [c] Average deviation between the $d_{calc} - d_{H_2O}$ (shown in column two of this table).

**Table II. Experimental Specific Volume of $D_2O$**

| Applied press, bar | 2°C | 4°C | 6°C | 8°C | 10°C | 12°C |
|---|---|---|---|---|---|---|
| 0.00 | 0.904966 | 0.904672 | 0.904471 | 0.904334 | 0.904268 | 0.904261 |
| 96.79 | 0.900401 | 0.900183 | 0.900049 | ... | 0.899964 | 0.900008 |
| 196.62 | 0.895844 | 0.895700 | 0.895631 | 0.895611 | 0.895659 | 0.895752 |
| 296.45 | 0.891434 | 0.891358 | 0.891351 | 0.891388 | 0.891489 | 0.891630 |
| 396.29 | 0.887178 | 0.887153 | 0.887203 | 0.887295 | 0.887443 | 0.887630 |
| 496.13 | 0.883033 | 0.883085 | 0.883182 | 0.883327 | 0.883521 | 0.883744 |
| 595.97 | 0.879039 | 0.879134 | 0.879290 | 0.879479 | 0.879716 | 0.879976 |
| 695.81 | 0.875162 | 0.875316 | 0.875520 | 0.875747 | 0.876018 | 0.876319 |
| 795.65 | 0.871411 | 0.871613 | 0.871854 | 0.872123 | 0.872435 | 0.872765 |
| 895.49 | 0.867779 | 0.868015 | 0.868299 | 0.868610 | 0.868952 | 0.869318 |
| 995.33 | 0.864250 | 0.864521 | 0.864855 | 0.865194 | 0.865572 | 0.865960 |
| Applied press, bar | 15°C | 20°C | 25°C | 30°C | 35°C | 40°C |
| 0.00 | 0.904365 | 0.904802 | 0.905541 | 0.906544 | 0.907799 | 0.909270 |
| 96.79 | 0.900179 | 0.900706 | 0.901518 | 0.902571 | 0.903858 | 0.905354 |
| 196.62 | 0.895991 | 0.896612 | 0.897491 | 0.898589 | 0.899914 | 0.901422 |
| 296.45 | 0.891928 | 0.892635 | 0.893578 | 0.894733 | 0.896087 | 0.897617 |
| 396.29 | 0.887984 | 0.888770 | 0.889778 | 0.890979 | 0.892362 | 0.893914 |
| 496.13 | 0.884160 | 0.885019 | 0.886087 | 0.887328 | 0.888755 | 0.890310 |
| 595.97 | 0.880441 | 0.881375 | 0.882499 | 0.883781 | 0.885225 | 0.886814 |
| 695.81 | 0.876834 | 0.877838 | 0.879004 | 0.880327 | 0.881800 | 0.883400 |
| 795.65 | 0.873326 | ... | 0.875602 | 0.876969 | 0.878461 | 0.880084 |
| 895.49 | 0.869913 | 0.871026 | 0.872301 | 0.873692 | ... | 0.876836 |
| 995.33 | 0.866594 | 0.867762 | 0.869076 | 0.870486 | 0.872032 | 0.873683 |

a nonweighted least-squares method) at each temperature to a linear function of pressure (*8*)

$$K = A_0' + A_1'P \quad (3)$$

where the constants $A_0'$ and $A_1'$ are functions of temperature. The coefficients for Equation 3 at each temperature are given in Table III along with the standard deviations. The standard deviations at each temperature are within 7 ppm.

Since a second degree secant bulk modulus equation is necessary to fit the specific volume data of water and seawater (*2, 5, 24*), we have also fit (using a nonweighted least-squares method) the $K$'s at each temperature to the equation

$$K = A_0 + A_1P + A_2P \quad (4a)$$

where the constants $A_0$, $A_1$, and $A_2$ are polynomial functions of temperature. The coefficients for Equation 4a at each temperature are given in Table III, along with the standard deviations. The coefficients for Equation 4a have also been determined by fitting (using a nonweighted least-squares method) all of the *PVT* data in a nonsequential manner. The coefficients $A_0$, $A_1$, and $A_2$ are given by

$$A_0 = 1.85823 \times 10^4 + 1.70680 \times 10^2t - 2.41402t^2 + 9.58993 \times 10^{-3}t^3 \quad (4b)$$

$$A_1 = 3.05748 - 5.51934 \times 10^{-3}t + 7.47238 \times 10^{-4}t^2 - 1.17862 \times 10^{-5}t^3 \quad (4c)$$

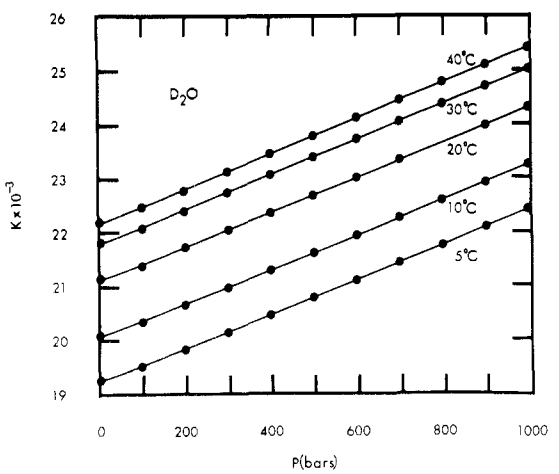


**Figure 1.** Secant bulk modulus of $D_2O$ at various temperatures plotted vs. pressure

$$A_2 = 1.80206 \times 10^{-4} + 2.37373 \times 10^{-6}t - 5.70772 \times 10^{-7}t^2 + 1.02188 \times 10^{-8}t^3 \quad (4d)$$

The standard deviations of Equation 4a at each temperature are within 2.7 ppm, whereas the overall equation has a standard deviation of 6 ppm. The residuals of the fitted equation of state Equation 4 and the experimental measurements showed no regular pressure or temperature dependencies (*3*) within the standard deviations of the fit. We feel that our results are accurate to within 3 $\sigma$ or 18 ppm over the range of our measurements.

Although a number of other equations of state could have been used to fit our *PVT* results, we have selected the second degree secant bulk modulus equation in this and other studies because it is easy to use, is an extension of the classical Tait equation (*22*), and fits the experimental *PVT* data and sound-derived data of seawater, $H_2O$, and $D_2O$ to within the experimental error of the measurements (*5, 6, 24*).

### Comparison of Results

The specific volumes determined at 1 atm in this study are compared to the results of Steckel and Szapiro (*20*) and Kell (*11*) in Table IV. Over most of the temperature range our results are 78–125 ppm lower than the results of Steckel and Szapiro (*20*) and Kell (*11*) for pure $D_2O$. This discrepancy is due to compositional differences in the $D_2O$ used in the two studies. If we assume that the differences between the density of $D_2O$ and $H_2O$ are linear in mole fraction (*15*), these density differences yield a mole fraction of 99.9% which is in good agreement with the actual value of 99.8%. Since we are only interested in determining the effect of pressure on the *PVT* properties of $D_2O$ in this paper (which is not strongly dependent upon the composition), we have selected to normalize our work to the 1 atm specific volume equation of state of Kell (*11*).

$$V^0 = (1 + 17.96190 \times 10^{-3}t)(1.104690 + 20.09315 \times 10^{-3}t - 9.24227 \times 10^{-6}t^2 - 55.9509 \times 10^{-9}t^3 + 79.9512 \times 10^{-12}t^4)^{-1} \quad (5)$$

The specific volumes at high pressures can be calculated from

$$V^P = V^0[1 - P/(A_0 + A_1P + A_2P^2)] \quad (6)$$

Values of $V^P$ at various pressures and temperatures calculated from Equation 6 (using the coefficients of 4 and 5) are given in Table V.

**Table III. Coefficients for Linear and Quadratic Secant Bulk Modulus Equations for $D_2O$ Along Isotherms**

| | Linear coeff | | Quadratic coeff | | | $\Delta V$, ppm[a] | |
|---|---|---|---|---|---|---|---|
| Temp, °C | $A_0$ | $A_1$ | $A_0$ | $A_1$ | $A_2 \times 10^3$ | Lin | Quad |
| 2 | 18861 | 3.2673 | 18881 | 3.1600 | 0.09943 | 7.1[a] | 1.9[a] |
| 4 | 19180 | 3.2563 | 19195 | 3.1793 | 0.07047 | 5.0 | 2.5 |
| 6 | 19471 | 3.2593 | 19488 | 3.1793 | 0.07914 | 5.2 | 1.6 |
| 8 | 19737 | 3.2720 | 19748 | 3.2249 | 0.03954 | 2.6 | 0.7 |
| 10 | 20012 | 3.2555 | 20024 | 3.1972 | 0.05330 | 3.1 | 0.9 |
| 12 | 20258 | 3.2513 | 20268 | 3.2013 | 0.04581 | 3.2 | 1.4 |
| 15 | 20593 | 3.2535 | 20596 | 3.2368 | 0.01526 | 1.1 | 1.1 |
| 20 | 21078 | 3.2539 | 21071 | 3.2902 | −0.03302 | 2.8 | 2.2 |
| 25 | 21475 | 3.2601 | 21471 | 3.2804 | −0.01860 | 1.7 | 1.5 |
| 30 | 21776 | 3.2833 | 21766 | 3.3366 | −0.05511 | 5.1 | 1.9 |
| 35 | 21983 | 3.3225 | 21964 | 3.4440 | −0.14150 | 6.8 | 1.9 |
| 40 | 22161 | 3.2922 | 22123 | 3.4275 | −0.10474 | 5.4 | 2.7 |
| | | | | | | Mean = 4.3 | 1.7 |

[a] $\Delta V = (V_{meas} - V_{calc})$ in parts per million and is the average deviation between the measured specific volumes in Table I and the specific volumes back-calculated from Equations 3a and 4a along each isotherm.

Although a number of workers (*1, 10, 13*) have studied the high-pressure *PVT* properties of $D_2O$, the only reliable high-pressure specific volume results appear to be those derived from the sound data of Wilson (*26*) by Fine and Millero (*6*). A comparison of the specific volumes obtained in this study and those derived by Fine and Millero (*6*) is shown in Figure 2. Over most of the *PT* space our measured results agree with the sound-derived data to within 40 ppm (which is approximately equivalent to the maximum error of 0.9 m $sec^{-1}$ in the sound data). The larger deviations at high pressures and temperatures (which also occur in our seawater work) are apparently due to calibration errors (*2, 3*).

**Table IV. Comparison of 1 Atm Specific Volume of $D_2O$ Obtained in This Study and by Other Workers**

| | $-\Delta V$, ppm | |
|---|---|---|
| Temp, °C | *a* | *b* |
| 2 | 86 | 102 |
| 4 | 78 | 91 |
| 6 | 86 | 97 |
| 8 | 86 | 95 |
| 10 | 90 | 97 |
| 12 | 92 | 98 |
| 15 | 95 | 100 |
| 20 | 99 | 104 |
| 25 | 105 | 112 |
| 30 | 107 | 119 |
| 35 | 119 | 135 |
| 40 | 125 | 145 |
| | Mean 97 | 108 |

[a] $\Delta V$ = $V$(measured) − $V$(Steckel and Szapiro). [b] $\Delta V$ = $V$(measured) − $V$(Kell). It should be pointed out that Kell's $V$'s for $D_2O$ are partly based on Steckel and Szapiro's results.

The high-pressure expansibilities of $D_2O$ can be obtained by differentiating Equation 6 with respect to temperature:

$$\alpha = \frac{1}{V^P}\left(\frac{\partial V^P}{\partial T}\right)_P = \frac{1}{V^P}\left(\frac{\partial V^0}{\partial T}\right) - \frac{P(\partial V^0/\partial T)}{V^P(A_0 + A_1P + A_2P^2)} + PV^0\frac{(\partial A_0/\partial T) + P(\partial A_1/\partial T) + P^2(\partial A_2/\partial T)}{V^P(A_0 + A_1P + A_2P^2)^2} \quad (7)$$

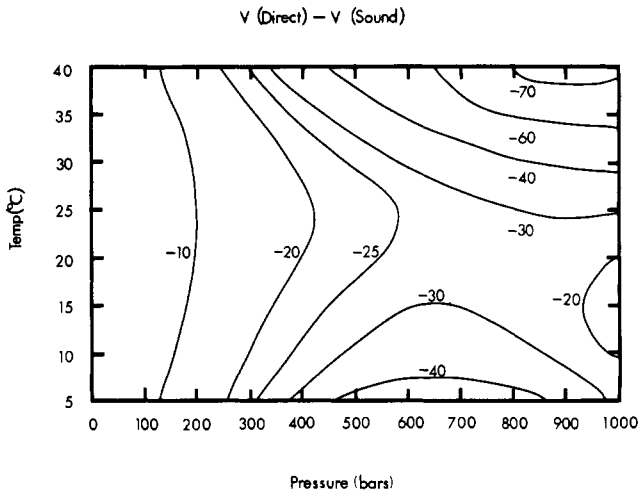


**Figure 2.** Contour diagram of differences in specific volumes of $D_2O$ obtained from our results and work of Fine and Millero from 5° to 40°C and 0 to 1000 bars (unit of contour is $1 \times 10^{-6}$ $cm^3$ $g^{-1}$)

**Table V. Calculated Specific Volume of $D_2O$ at Various Pressures and Temperatures (Equation 6)**

| Applied press | 5°C | 10°C | 15°C | 20°C | 25°C | 30°C | 35°C | 40°C |
|---|---|---|---|---|---|---|---|---|
| 0 | 0.904468 | 0.904171 | 0.904265 | 0.904698 | 0.905429 | 0.906425 | 0.907664 | 0.909125 |
| 100 | 0.899873 | 0.899731 | 0.899948 | 0.900475 | 0.901277 | 0.902326 | 0.903601 | 0.905083 |
| 200 | 0.895420 | 0.895425 | 0.895758 | 0.896376 | 0.897247 | 0.898346 | 0.899655 | 0.901156 |
| 300 | 0.891106 | 0.891248 | 0.891691 | 0.892395 | 0.893332 | 0.894480 | 0.895821 | 0.897342 |
| 400 | 0.886926 | 0.887198 | 0.887743 | 0.888529 | 0.889529 | 0.890723 | 0.892095 | 0.893634 |
| 500 | 0.882876 | 0.883269 | 0.883912 | 0.884774 | 0.885833 | 0.887070 | 0.888473 | 0.890029 |
| 600 | 0.878953 | 0.879459 | 0.880192 | 0.881125 | 0.882239 | 0.883518 | 0.884949 | 0.886523 |
| 700 | 0.875153 | 0.875763 | 0.876580 | 0.877580 | 0.878746 | 0.880063 | 0.881521 | 0.883111 |
| 800 | 0.871471 | 0.872179 | 0.873073 | 0.874135 | 0.875347 | 0.876700 | 0.878184 | 0.879791 |
| 900 | 0.867906 | 0.868702 | 0.869668 | 0.870785 | 0.872041 | 0.873427 | 0.874934 | 0.876558 |
| 1000 | 0.864452 | 0.865331 | 0.866361 | 0.867529 | 0.868824 | 0.870239 | 0.871769 | 0.873410 |

**Table VI. Calculated Expansibility of $D_2O$ at Various Pressures and Temperatures (Equation 7)**
$\alpha \times 10^6$ ($deg^{-1}$)

| Applied press | 5°C | 10°C | 15°C | 20°C | 25°C | 30°C | 35°C | 40°C |
|---|---|---|---|---|---|---|---|---|
| 0 | −114.1 | −20.1 | 60.1 | 129.9 | 191.8 | 247.4 | 298.1 | 344.8 |
| 100 | −75.9 | 10.4 | 84.3 | 148.8 | 206.3 | 258.2 | 305.6 | 349.4 |
| 200 | −39.6 | 39.5 | 107.5 | 167.2 | 220.4 | 268.7 | 312.9 | 353.8 |
| 300 | −5.3 | 67.3 | 129.8 | 184.9 | 234.1 | 278.8 | 319.9 | 358.0 |
| 400 | 27.1 | 93.6 | 151.1 | 201.8 | 247.3 | 288.7 | 326.8 | 362.2 |
| 500 | 57.7 | 118.5 | 171.2 | 217.9 | 259.8 | 298.1 | 333.4 | 366.3 |
| 600 | 86.5 | 142.0 | 190.3 | 233.1 | 271.7 | 307.1 | 339.9 | 370.4 |
| 700 | 113.5 | 164.0 | 208.1 | 247.4 | 283.0 | 315.7 | 346.1 | 374.6 |
| 800 | 138.8 | 184.6 | 224.7 | 260.7 | 293.5 | 323.8 | 352.2 | 378.9 |
| 900 | 162.4 | 203.7 | 240.1 | 272.9 | 303.2 | 331.5 | 358.1 | 383.5 |
| 1000 | 184.4 | 221.3 | 254.1 | 284.2 | 312.2 | 338.6 | 363.9 | 388.2 |

Values of $\alpha$ determined from Equation 7 at various pressures and temperatures are given in Table VI. A comparison of the $\alpha$'s given in Table VI and those obtained from the sound-generated equation of state of Fine and Millero is shown in Figure 3. Over the entire $PT$ space, our directly measured $\alpha$'s agree with the sound-derived data to within ±4 ppm.

The isothermal compressibility of $D_2O$ can be obtained by differentiating Equation 6 with respect to pressure:

$$\beta = \frac{-1}{V^P}\left(\frac{\partial V^P}{\partial P}\right) = \frac{V^0(A_0 - A_2P^2)}{V^P(A_0 + A_1P + A_2P)^2} \qquad (8)$$

Values of $\beta$ determined from this equation at various temperatures and pressures are given in Table VII. At $P$ = 0 or 1 atm these results are compared in Table VIII to the directly measured results of Millero and Lepple (*17*) and the sound-derived results of Fine and Millero (*6*). Over the entire temperature range, our results are in agreement with those determined by others workers to within $0.12 \times 10^{-6}$ bar$^{-1}$ (av dev is $\pm 0.07 \times 10^{-6}$ bar$^{-1}$).

A comparison of the high-pressure compressibilities obtained in this study are shown in Figure 4. Over the entire $PT$ space, our derived $\beta$'s agree with the sound-derived data to within 0.1 ppm.

In summary, our derived $PVT$ data agree with the sound-derived data to within $\pm 70 \times 10^{-6}$ in $V^P$, $\pm 3 \times 10^{-6}$ in $\alpha^P$, and $\pm 0.1 \times 10^{-6}$ in $\beta^P$.

The high-pressure $PVT$ properties of $D_2O$ determined from our results and $H_2O$ from the work of Fine and Millero from 5° to 45°C and 0 to 1000 bars applied pressure have been made elsewhere (*2*). These comparisons indicate that as the temperature is increased, the derivatives $(\partial V/\partial T)_P$, $(\partial V/\partial P)_T$, $(\partial^2 V/\partial T^2)_P$, and $(\partial T/\partial P)_S = (T/C_p)(\partial V/\partial T)_P$ of $D_2O$ and $H_2O$ approach each other over the entire pressure range. At lower temperatures these derivatives are more temperature dependent in $D_2O$ than $H_2O$ which indicates that $D_2O$ is more structured than $H_2O$. The heat capacities at constant pressure ($C_p$) at 1 atm for $D_2O$ (*4*) and $H_2O$ (*21*) also approach each other at higher temperatures; however, the values of $C_p$ at high pressures for $D_2O$ and $H_2O$ derived from

$$C_p(P) = C_p(0) - T\int_0^P (\partial^2 V/\partial T^2)dP \qquad (9)$$

are relatively parallel to one another and not strongly affected by temperature. The heat capacities at constant volume of $D_2O$ and $H_2O$ decrease with increasing temperature (at higher pressures the decrease is smaller). Over the entire pressure range the $C_v$ of both $D_2O$ and $H_2O$ are nearly parallel, although there is an indication that they approach each other at the fusion line.

The specific heats of both $D_2O$ and $H_2O$ decrease with an increase in pressure. At low temperature the decrease in $C_p$ and $C_v$ is greater for $D_2O$ than $H_2O$; at higher temperatures the decrease of $C_p$ with increasing pressure for $D_2O$ and $H_2O$ appears to be similar. Owing to possible "end effects" in the temperature fits at low temperatures, we cannot at present be certain that the values for the effect of pressure on the $C_p$ are reliable. The pressure dependence for the $C_p$ of $H_2O$ determined from the equation of state of Fine and Millero is in excellent agreement (*3*) with the directly measured values of Sirota et al. (*19*) at 0°C—indicating that, at least for $H_2O$, the

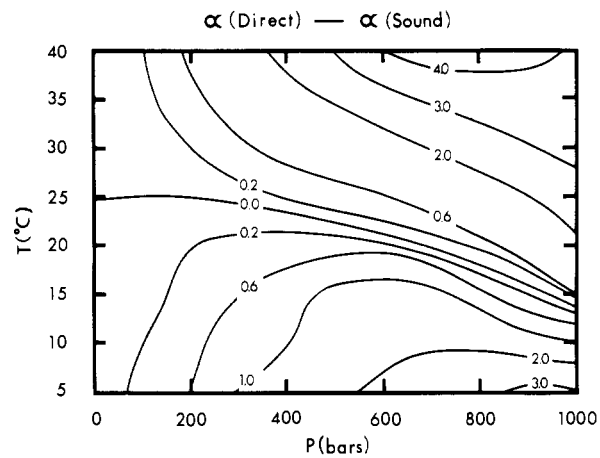


**Figure 3.** Contour diagram of differences in expansibilities of $D_2O$ obtained from our results and work of Fine and Millero from 5° to 40°C and 0 to 1000 bars (unit of contour is $1 \times 10^{-6}$ deg$^{-1}$)

**Table VIII. Comparisons of 1 Atm Compressibilities Obtained by Various Workers**

$\Delta\beta \times 10^6$ (bar$^{-1}$)

| Temp, °C | *a* | *b* |
|---|---|---|
| 5 | 0.12 | 0.06 |
| 10 | 0.12 | 0.06 |
| 15 | 0.09 | 0.05 |
| 20 | 0.01 | 0.05 |
| 25 | 0.01 | 0.05 |
| 30 | 0.02 | 0.05 |
| 35 | 0.06 | 0.05 |
| 40 | 0.03 | 0.05 |

[a] $\beta$(Our results) − $\beta$(Millero and Lepple). [b] $\beta$(Our results) − $\beta$(Fine and Millero).

**Table VII. Calculated Compressibility of $D_2O$ at Various Pressures and Temperatures (Equation 8)**

$\beta \times 10^6$ (bar$^{-1}$)

| Applied press | 5°C | 10°C | 15°C | 20°C | 25°C | 30°C | 35°C | 40°C |
|---|---|---|---|---|---|---|---|---|
| 0 | 51.61 | 49.86 | 48.47 | 47.38 | 46.53 | 45.89 | 45.43 | 45.12 |
| 100 | 50.26 | 48.59 | 47.26 | 46.20 | 45.38 | 44.76 | 44.31 | 44.01 |
| 200 | 48.95 | 47.36 | 46.08 | 45.06 | 44.27 | 43.66 | 43.23 | 42.94 |
| 300 | 47.65 | 46.15 | 44.93 | 43.96 | 43.19 | 42.61 | 42.18 | 41.91 |
| 400 | 46.39 | 44.96 | 43.81 | 42.88 | 42.15 | 41.59 | 41.18 | 40.91 |
| 500 | 45.15 | 43.80 | 42.71 | 41.83 | 41.14 | 40.60 | 40.21 | 39.94 |
| 600 | 43.93 | 42.67 | 41.64 | 40.81 | 40.16 | 39.65 | 39.27 | 39.01 |
| 700 | 42.74 | 41.56 | 40.60 | 39.82 | 39.21 | 38.73 | 38.37 | 38.11 |
| 800 | 41.57 | 40.47 | 39.58 | 38.86 | 38.29 | 37.84 | 37.49 | 37.24 |
| 900 | 40.43 | 39.41 | 38.58 | 37.92 | 37.40 | 36.98 | 36.65 | 36.39 |
| 1000 | 39.32 | 38.37 | 37.61 | 37.01 | 36.53 | 36.15 | 35.84 | 35.57 |

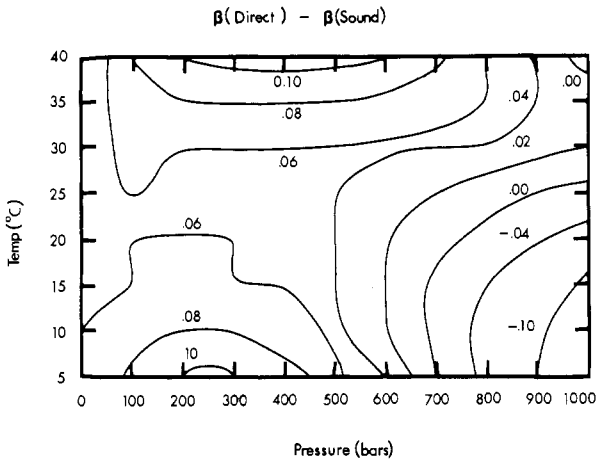


**Figure 4.** Contour diagram of differences in compressibilities of $D_2O$ obtained from our results and work of Fine and Millero from 5° to 40°C and 0 to 1000 bars (unit of contour is $1 \times 10^{-6}$ $bar^{-1}$)

secant bulk modulus equation does not have large "end effects." Since our measurements on $D_2O$ were made relative to the equation of state for $H_2O$ of Fine and Millero, the high-pressure specific heats of $D_2O$ determined from our equation of state are probably of reasonable validity. High-pressure specific heat measurements on $D_2O$ similar to those of Sirota et al. (*19*) would prove or disprove these speculations.

Since the specific heats of liquids are directly related to the molecular structure of a liquid, the high-pressure values of $C_p$ and $C_v$ for $D_2O$ calculated from our equation of state may be useful in elucidating the structure of water.

## Literature Cited


(1) Bridgman, P. W., *J. Chem. Phys.*, **3**, 597 (1935).
(2) Emmet, R. T., Millero, F. J., *J. Geophys. Res.*, **79**, 3463 (1974).
(3) Emmet, R. T., PhD thesis, University of Miami, Miami, Fla., 1973.
(4) Eucken, A., Eigen, M., *Z. Elektro. Chem.*, **55**, 343 (1951).
(5) Fine, R. A., Millero, F. J., *J. Chem. Phys.*, **59**, 5529 (1973).
(6) Fine, R. A., Millero, F. J., *ibid.*, **63**, 89 (1975).
(7) Frank, H. S., in "Water," p 542, F. Franks, Ed., Plenum Press, New York, N.Y., 1972.
(8) Hayward, A.T.J., *Brit. J. Appl. Phys.*, **18**, 965 (1967).
(9) Jhons, M. S., Grosh, J., Ree, T., Eyring, H., *J. Chem. Phys.*, **44**, 1465 (1966).
(10) Jůza, J., Kmonicek, V., Sifner, O., Schovanec, K., *Physica*, **32**, 362 (1966).
(11) Kell, G. S., *J. Chem. Eng. Data*, **12**, 66 (1967).
(12) Kesselman, P. M., *Teploenergetika*, **3**, 83 (1960).
(13) Kesselman, P. M., *ibid.*, **4**, 72 (1960).
(14) Millero, F. J., *Rev. Sci. Instrum.*, **38**, 1441 (1967).
(15) Millero, F. J., Hoff, E. V., Dexter, R., *J. Chem. Eng. Data*, **16**, 85 (1971).
(16) Millero, F. J., Knox, J. H., Emmet, R. T., *J. Solution Chem.*, **1**, 173 (1972).
(17) Millero, F. J., Lepple, F. K., *J. Chem. Phys.*, **54**, 946 (1971).
(18) Nemethy, G., Schraga, H. A., *ibid.*, **41**, 680 (1964).
(19) Sirota, A. M., Grishkov, A. Ya., Tomishko, A. G., *Teploenergetika*, **17**, 60 (1970).
(20) Steckel, F., Szapiro, S., *Trans. Faraday Soc.*, **59**, 331 (1963).
(21) Stimson, H. F., *Am. J. Phys.*, **23**, 614 (1955).
(22) Tait, P. G., "The Voyage of H.M.S. Challenger," 73 pp, II HMSO, London, England, 1888.
(23) Walrafen, G. E., in "Water," F. Franks, Ed., Plenum Press, New York, N.Y., 1972.
(24) Wang, D. P., Millero, F. J., *J. Geophys. Res.*, **78**, 7122 (1973).
(25) Weres, O., Rice, S. A., *J. Am. Chem. Soc.*, **94**, 8983 (1962).
(26) Wilson, W. D., *J. Acoust. Soc. Am.*, **33**, 314 (1961).



Received for review October 10, 1974. Accepted May 27, 1975. Research supported by the Office of Naval Research (N00014-67-A-0201-0013) and the Oceanographic Branch of the National Science Foundation (GA-17386 and GA-40532). R.T.E. supported by Navships Ocean Science Program during analysis and write-up of results. Paper taken in part from dissertation submitted by R.T.E. in partial fulfillment of the requirements for the PhD, University of Miami.


# Effects of Temperature and Pressure on Conductance of Solid Electrolyte, $RbAg_4I_5$


**Kyung S. Kim[1] and Woon-kie Paik[2]**
*Department of Chemistry, Sogang University, Seoul, Korea*



**The effects of temperature and pressure on ionic conductance of the solid electrolyte, $RbAg_4I_5$, were investigated. The potential probe method was used in measuring the conductance with ac current imposed on the specimen to avoid contact resistance and polarization effects between the sample and the current supplying electrodes. The specific conductance, $\sigma$, was 0.288 $ohm^{-1}$ $cm^{-1}$ at 25°C, and the activation energy was calculated to be 1.59 kcal/mol of $Ag^+$. The specific conductance increased as the pressure increased up to 8000 kg $cm^{-2}$. From the increase of $\sigma$ with pressure and the compressibility data, an activation volume of −0.32 $cm^3$/mol of $Ag^+$ was obtained by the absolute reaction rate theory applied to the electrochemical process.**


There has been considerable interest in solid electrolytes owing to recent discoveries of their highly conducting nature and of their wide range of applications (*8, 10, 11, 20, 21*). Compounds of the type $MAg_4I_5$ in which M is $K^+$, $Rb^+$, or $NH_4^+$ have high ionic conductance in the solid state owing to the exceptionally mobile $Ag^+$ ions (*2*). Rubidium silver iodide, $RbAg_4I_5$, is the most stable among these. Consequently, much attention has been focused on this electrolyte. In $RbAg_4I_5$, 16 $Ag^+$ ions which have high mobility are statistically distributed over 56 available tetrahedral sites per unit cell (*5*). Each of these tetrahedral sites has four $I^-$ ions at its apexes.

Although the conductance of $RbAg_4I_5$ has been reported by several authors (*2, 4, 12, 16, 17*), the data are scattered, ranging from 0.124 to 0.279 $ohm^{-1}$ $cm^{-1}$, depending upon the experimental methods used (*17*). This scatter of data indicates that measuring techniques did not completely exclude contact resistance and polarization effects between samples and current-supplying electrodes, in spite of many efforts to avoid this problem (*12, 16, 17*). With aqueous solutions the


[1] Present address, Department of Chemistry, State University of New York at Stony Brook, Stony Brook, N.Y.
[2] To whom correspondence should be addressed.